Measurement of the ^{236}U(n,f) cross section from 170 meV to 2 MeV at the CERN n_TOF facility

R. Sarmento,[1] M. Calviani,[2] J. Praena,[14] N. Colonna,[3] F. Belloni,[4] I. F. Gonçalves,[1] P. Vaz,[1] G. Aerts,[17] H. Alvarez,[26] F. Alvarez-Velarde,[5] S. Andriamonje,[2] J. Andrzejewski,[6] P. Assimakopoulos,[7] L. Audouin,[8] M. Barbagallo,[3] G. Badurek,[9] P. Baumann,[10] F. Becvar,[11] E. Berthoumieux,[17] F. Calvino,[12] D. Cano-Ott,[5] R. Capote,[13,14] C. Carrapiço,[1] A. Carrillo de Albornoz,[1] P. Cennini,[15] V. Chepel,[16] E. Chiaveri,[2] G. Cortes,[18] A. Couture,[19] J. Cox,[19] M. Dahlfors,[15] S. David,[8] M. Diakaki,[34] I. Dillmann,[20] R. Dolfini,[21] C. Domingo-Pardo,[22] W. Dridi,[17] I. Duran,[26] C. Eleftheriadis,[23] L. Ferrant,[8] A. Ferrari,[15] R. Ferreira-Marques,[16] H. Frais-Koelbl,[13] K. Fuji,[4] W. Furman,[24] E. Gonzalez-Romero,[5] A. Goverdovski,[25] F. Gramegna,[15] E. Griesmayer,[13] C. Guerrero,[5,2] F. Gunsing,[17] B. Haas,[27] R. Haight,[28] M. Heil,[20] A. Herrera-Martinez,[15] M. Igashira,[29] S. Isaev,[8] E. Jericha,[9] F. Käppeler,[20] Y. Kadi,[15] D. Karadimos,[7] D. Karamanis,[6] M. Kerveno,[10] V. Ketlerov,[25] P. Koehler,[30] V. Konovalov,[24] E. Kossionides,[31] M. Krticka,[11] C. Lampoudis,[23,17] C. Lederer,[35] H. Leeb,[9] A. Lindote,[16] I. Lopes,[16] M. Lozano,[14] S. Lukic,[10] J. Marganiec,[6] L. Marques,[1] S. Marrone,[3] T. Martinez,[5] C. Massimi,[32] P. Mastinu,[15] E. Mendoza,[5] A. Mengoni,[13,39] P. M. Milazzo,[4] C. Moreau,[4] M. Mosconi,[20] F. Neves,[16] H. Oberhummer,[9] S. O'Brien,[19] M. Oshima,[33] J. Pancin,[17] C. Papachristodoulou,[7] C. Papadopoulos,[34] C. Paradela,[26] N. Patronis,[7] A. Pavlik,[35] P. Pavlopoulos,[36] L. Perrot,[17] M. T. Pigni,[9] R. Plag,[20] A. Plompen,[37] A. Plukis,[17] A. Poch,[18] C. Pretel,[18] J. Quesada,[14] T. Rauscher,[38] R. Reifarth,[28] M. Rosetti,[39] C. Rubbia,[21] G. Rudolf,[10] P. Rullhusen,[37] J. Salgado,[1] L. Sarchiapone,[15] I. Savvidis,[23] C. Stephan,[8] G. Tagliente,[3] J. L. Tain,[22] D. Tarrio,[26] L. Tassan-Got,[8] L. Tavora,[1] R. Terlizzi,[3] G. Vannini,[32] A. Ventura,[39] D. Villamarin,[5] M. C. Vicente,[5] V. Vlachoudis,[2] R. Vlastou,[34] F. Voss,[20] S. Walter,[20] H. Wendler,[15] M. Wiescher,[19] and K. Wisshak[20]

(The n_TOF Collaboration)

[1]*Instituto Tecnológico e Nuclear (ITN), Sacavém, Portugal*

[2]*European Organization for Nuclear Research (CERN), Geneva, Switzerland*

[3]*Istituto Nazionale di Fisica Nucleare (INFN), Bari, Italy*

[4]*Istituto Nazionale di Fisica Nucleare (INFN), Trieste, Italy*

[5]*Centro de Investigaciones Energeticas Medioambientales y Technologicas CIEMAT, Madrid, Spain*

[6]*University of Lodz, Lodz, Poland*

[7]*University of Ioannina, Greece*

[8]*Centre National de la Recherche Scientifique/IN2P3 - IPN, Orsay, France*

[9]*Atominstitut der Osterreichischen Universitäten, Techn. Universität Wien, Austria*

[10]*Centre National de la Recherche Scientifique/IN2P3 - IReS, Strasbourg, France*

[11]*Charles University, Prague, Czech Republic*

[12]*Universidad Politecnica de Madrid, Spain*

[13]*International Atomic Energy Agency (IAEA), Nuclear Data Sect., Vienna, Austria*

[14]*Universidad de Sevilla, Spain*

[15]*Istituto Nazionale di Fisica Nucleare (INFN), Laboratori Nazionali di Legnaro, Italy*

[16]*LIP - Coimbra e Departamento de Fisica da Universidade de Coimbra, Portugal*

[17]*CEA/Saclay - DSM/Irfu, Gif-sur-Yvette, France*

[18]*Universitat Politecnica de Catalunya, Barcelona, Spain*

[19]*University of Notre Dame, Notre Dame, Indiana, USA*

[20]*Karlsruhe Institute of Technology (KIT), Campus Nord, Institute of Nuclear Physics, Karlsruhe, Germany*

[21]*Universita degli Studi Pavia, Pavia, Italy*

[22]*Instituto de Fsica Corpuscular, CSIC-Universidad de Valencia, Spain*

[23]*Aristotle University of Thessaloniki, Greece*

[24]*Joint Institute for Nuclear Research, Frank Lab. Neutron Physics, Dubna, Russia*

[25]*Institute of Physics and Power Engineering, Kaluga region, Obninsk, Russia*

[26]*Universidade de Santiago de Compostela, Spain*

[27]*Centre National de la Recherche Scientifique/IN2P3 - CENBG, Bordeaux, France*

[28]*Los Alamos National Laboratory, New Mexico, USA*

[29]*Tokyo Institute of Technology, Tokyo, Japan*

[30]*Oak Ridge National Laboratory, Physics Division, Oak Ridge, Tenessee, USA*

[31]*NCSR, Athens, Greece*

[32]*Dipartimento di Fisica, Universita di Bologna, and Sezione INFN di Bologna, Italy*

[33]*Japan Atomic Energy Research Institute, Tokaimura, Japan*

[34]*National Technical University of Athens, Greece*

[35]*Institut fur Isotopenforschung und Kernphysik, Universität Wien, Austria*

[36]*Pole Universitaire Leonard de Vinci, Paris La Defense, France*

[37]*CEC-JRC-IRMM, Geel, Belgium*

[38]*Department of Physics and Astronomy - University of Basel, Basel, Switzerland*

[39]*ENEA, Bologna, Italy*

(Received 4 August 2011; published 31 October 2011)

The neutron-induced fission cross section of ^{236}U was measured at the neutron Time-of-Flight (n_TOF) facility at CERN relative to the standard ^{235}U(n,f) cross section for neutron energies ranging from above thermal to several MeV. The measurement, covering the full range simultaneously, was performed with a fast ionization chamber, taking advantage of the high resolution of the n_TOF spectrometer. The n_TOF results confirm that the first resonance at 5.45 eV is largely overestimated in some nuclear data libraries. The resonance triplet around 1.2 keV was measured with high resolution and resonance parameters were determined with good accuracy. Resonances at high energy have also been observed and characterized and different values for the cross section are provided for the region between 10 keV and the fission threshold. The present work indicates various shortcomings of the current nuclear data libraries in the subthreshold region and provides the basis for an accurate re-evaluation of the ^{236}U(n,f) cross section, which is of great relevance for the development of emerging or innovative nuclear reactor technologies.

DOI: 10.1103/PhysRevC.84.044618 PACS number(s): 25.85.Ec

I. INTRODUCTION

The sustainability of nuclear energy and the need to address issues such as better economics of the nuclear fuel cycle, proliferation resistance, improved safety, and reduced production of waste with high radiotoxicity stresses the need for an accurate determination of the neutron-induced cross sections of several actinides. New data are needed for advanced reactors based on the U/Pu cycle, as well as for the development of nuclear systems based on the Th/U cycle [1].

The nucleus ^{236}U builds up in the equilibrium state of the Th/U fuel cycle and its fission cross section is required with 5% accuracy for the development of fast nuclear reactors and accelerator-driven systems [2]. Below and at the fission threshold the available Evaluated Nuclear Data File (ENDF/B-VII.0), Joint Evaluated Fission and Fusion File (JEFF)-3.1, and Japanese Evaluated Nuclear Data Library (JENDL)-3.3 evaluations of the ^{236}U(n,f) cross section show significant discrepancies of up to one order of magnitude [3–5].

The first reported measurement of the ^{236}U(n,f) cross section was performed in a survey of the fission properties of the actinides [6], yielding a rather uncertain value of 1.8 ± 1.1 b at 14 MeV due to the low ^{236}U enrichment of the sample. This result was improved in later measurements at Los Alamos National Laboratory (LANL) [7,8], where the fission threshold of the reaction was found to be around 690 keV with a value of 0.04 ± 0.08 b [7]. Using a tritium gas target for neutron production at Oak Ridge National Laboratory (ORNL), the cross section at and above the threshold was further improved reaching an accuracy of 5.3% [9,10].

A later measurement dedicated to the systematics of the fission process was performed at the occasion of the Pommard nuclear explosion event at LANL [11]. From this study, cross-section data were obtained from 35.2 eV to 2 keV and from 100 keV to 2.935 MeV. The ^{236}U sample was placed at a flight path of 214.4 m and contained an impurity of 0.15% ^{235}U, which was neglected in the data analysis. Furthermore, a 40% disagreement in the cross-section data was found from independent readings at angles of 55 and 90 deg. As no explanation was found, the average was adopted for the final cross sections.

The widths and spacings of the subthreshold resonances were investigated by Theobald *et al.* [12] to determine the parameters of the double-humped fission barrier of ^{237}U. The measurement was performed up to 1 keV neutron energy using the pulsed neutron beam of the Institute for Reference Materials and Measurements (IRMM) at Geel at a flight path of 30 m and a ^{236}U sample containing only 0.2% of ^{235}U. Sixteen fission resonances were found between 5 and 415 eV. The deduced resonance parameters were used as a reference for the ENDF, JEFF, and JENDL evaluations of the ^{236}U(n,f) cross section [3–5].

In a parallel attempt, Schmitt *et al.* [13] used the 33 m flight path at the Oak Ridge Electron Linear Accelerator (ORELA) to study the structures in the cross section around the fission threshold. The energy resolution obtained in this experiment was 0.7% at 1 MeV. The data were normalized to 0.805 b at 2 MeV, and the peaks found at 0.75 MeV, 0.95 MeV, 1.15 MeV, 1.3 MeV, and 1.4 MeV were suggested to arise from collective levels. In subsequent experiments by Behrens and Carlson [14], Meadows [15], and Manabe *et al.* [16] the investigated energy range could be extended up to 14.74 MeV.

Stimulated by the fact that the cross section reported by Cramer and Berger [11] was a factor of 30 lower than the value obtained from the resonance parameters of Theobald *et al.* [12], Parker *et al.* [17] remeasured the ^{236}U(n,f) cross section at the Los Alamos Neutron Science Center (LANCSE) facility at LANL. In this experiment most previously reported fission resonances could be shown to result either from ^{235}U impurities in the sample or were overestimated due to γ-sensitive detectors. Apart from the 5.45 eV resonance, four newly observed well-separated resonance groups were identified between 1 and 12 keV. More recently, Wagemans *et al.* [18] measured the thermal fission cross section of ^{236}U at the Institut Laue-Langevin (ILL) in Grenoble, using a very pure ^{236}U sample with only 0.0043% ^{235}U. The cross section at thermal energy was found to be 0.3 ± 1.0 mb, consistent with the results of Parker *et al.*

In a second measurement Wagemans *et al.* [19] determined the cross section at the Geel Electron Linear Accelerator (GELINA) facility at JRC-IRMM from 500 meV up to 25 keV, emphasizing that the accuracy of the ^{236}U cross section affects the radioactive nuclear waste as well as the neutron balance in nuclear fuel cycles. Using the same very pure ^{236}U sample of Ref. [18], the results of Parker *et al.* for the 5.45 eV resonance as well as for the resonance clusters in the keV

region were confirmed, although the resonances could not be well resolved due to the short 8.3 m flight path. The analysis of the 5.45 eV resonance yielded a width of 1.7 ± 0.1 μeV, two orders of magnitude lower than claimed by ENDF/B-VII.0, JEFF-3.1, and JENDL-3.3. The Breit-Wigner extrapolation of the resonance tail yielded a thermal cross section consistent with the previously measured value, two orders of magnitude lower than given in the data libraries.

Recently, Alekseev *et al.* [20] measured the ^{236}U(n,f) cross section up to 20 keV with a lead slowing-down spectrometer in a joint experiment of the Institute for Nuclear Research (INR) at Moscow and the Institute of Physics and Power Engineering (IPPE) at Obninsk. Resonance parameters were provided at 5.45 eV and 1.28 keV with fission widths below those in Refs. [17,19]. After subtraction of the ^{235}U contamination yield, they observed no resonances in the tens- and hundreds-of-eV region. From the lack of structure in this region they concluded that the measurement of the small ^{236}U(n,f) cross-section value was only made possible by directly detecting the fission fragments.

In summary, the most recent measurements point out several problems in current evaluations. In particular, issues that need to be clarified are the thermal cross section value, the width of the 5.45 eV resonance, the origin of the resonances in the energy region between 29 and 415 eV, the presence and strength of intermediate-energy resonance structures above 1 keV and, finally, the value of the cross section in the unresolved resonance region. The origin of most of such shortcomings is related to the poor quality of the early experimental data below the fission threshold (690 keV), on which evaluations are still based. Above this value, there are several absolute cross-section measurements and measurements relative to the ^{235}U(n,f) cross section performed up to 20 MeV which are in good agreement with each other [9,10,14,15,21–24]. As a consequence, the evaluated cross sections above the fission threshold are more accurate, with small differences between the various databases.

In view of the discrepancies in the fission cross-section data of ^{236}U in the subthreshold region, a new measurement was performed at the neutron Time-Of-Flight facility (n_TOF) at CERN, Geneva [25,26]. The aim of the measurement was to extract a consistent set of high-resolution, high-accuracy data from thermal energies to a few MeV, thus providing the basis for a new evaluation to be used in the field of nuclear power technologies. The paper is organized as follows: after a brief introduction on the n_TOF facility and experimental apparatus in Sec. III, the analysis procedure is described in Sec. IV. Results are reported in Sec. V together with a comparison with previous data and with current evaluations.

II. EXPERIMENTAL SETUP

A. Neutron time-of-flight spectrometer at CERN

The neutron beam at n_TOF is produced by 20 GeV/c protons impinging onto an $80 \times 80 \times 60$ cm^3 $^{\text{nat}}$Pb spallation target. Proton bunches with 7 ns width (rms) and a repetition rate lower than 0.8 Hz were delivered by the CERN Proton Synchrotron. A 5.8-cm-thick water layer around the spallation target served as coolant and as a neutron moderator, resulting in a wide spectrum ranging from thermal energies up to a few GeV [25]. The experimental area located at the end of a 182.5-m-long tunnel is connected with the spallation target by an evacuated beam tube. The short proton pulse width combined with the long flight path results in high resolution in neutron energy, which is required for studying cross-section resonances. The neutron beam profile is shaped by two collimators in the beam tube, providing a diameter of 8 cm at the entrance of the experimental area. The spatial beam profile is flat in the sample region; in particular, above 1 eV. For each pulse of 7×10^{12} protons impinging on the spallation target, more than 2.5×10^{5} neutrons per energy decade reach the experimental area. In order to reduce the background from the spallation process, the TOF tube is tilted at a 10 $^\circ$ angle relative to the proton-beam direction. The ambient background in the experimental area is strongly reduced by massive concrete and iron shieldings along the flight path and by a sweeping magnet at 135 m.

B. Detector and data acquisition

The multistack fast ionization chamber, which was used in the measurement, has been described in detail in Ref. [27]. The chamber was operated as a closed system with a gas mixture of 90% Ar and 10% CF_4 at a pressure of 720 mbar. The case and windows of the detector are made of stainless steel. Inside the detector, a stack of ionization chambers is mounted along the direction of the neutron beam. Each cell consists of a central aluminum electrode 100 μm thick, which was plated on both sides with the isotope to be measured, and two external 15-μm-thick aluminum electrodes. The 20-mm-wide gap between electrodes was sufficient to stop the fission fragments, thus producing much bigger signals than those of α particles from the radioactive decay or from the competing (n,α) and (n,p) reactions above 50 keV.

A scheme of the detector is shown in Fig. 1. The solid angle of detection is very close to 2π and the efficiency for a fission event is almost 100%. The total detection efficiency was obtained by detailed FLUKA simulations of the energy deposition in the gas as a function of the threshold used in data analysis [28]. The detector was positioned in the experimental area 186.4 m downstream of the spallation target. Two ^{235}U and four ^{236}U samples were mounted inside the chamber. The detector signals were amplified by a current feedback operational amplifier AD844 and digitized with a flash analog-to-digital converter (ADC) with 8-bit resolution and 250 MHz sampling rate [29]. The fast timing properties of the gas and of the front-end electronics result in a fast signal. The digitized waveform produced by a fission fragment shows typically a rise time of 40 ns and a fall time of 120 ns. The raw data were stored in the CERN central advanced storage (CASTOR) manager after the application of zero-suppression and compression algorithms.

C. Samples

The ^{235}U and ^{236}U samples used for the measurement were in the form of U_3O_8 deposits 80 mm in diameter. The masses of the samples were determined by α counting and

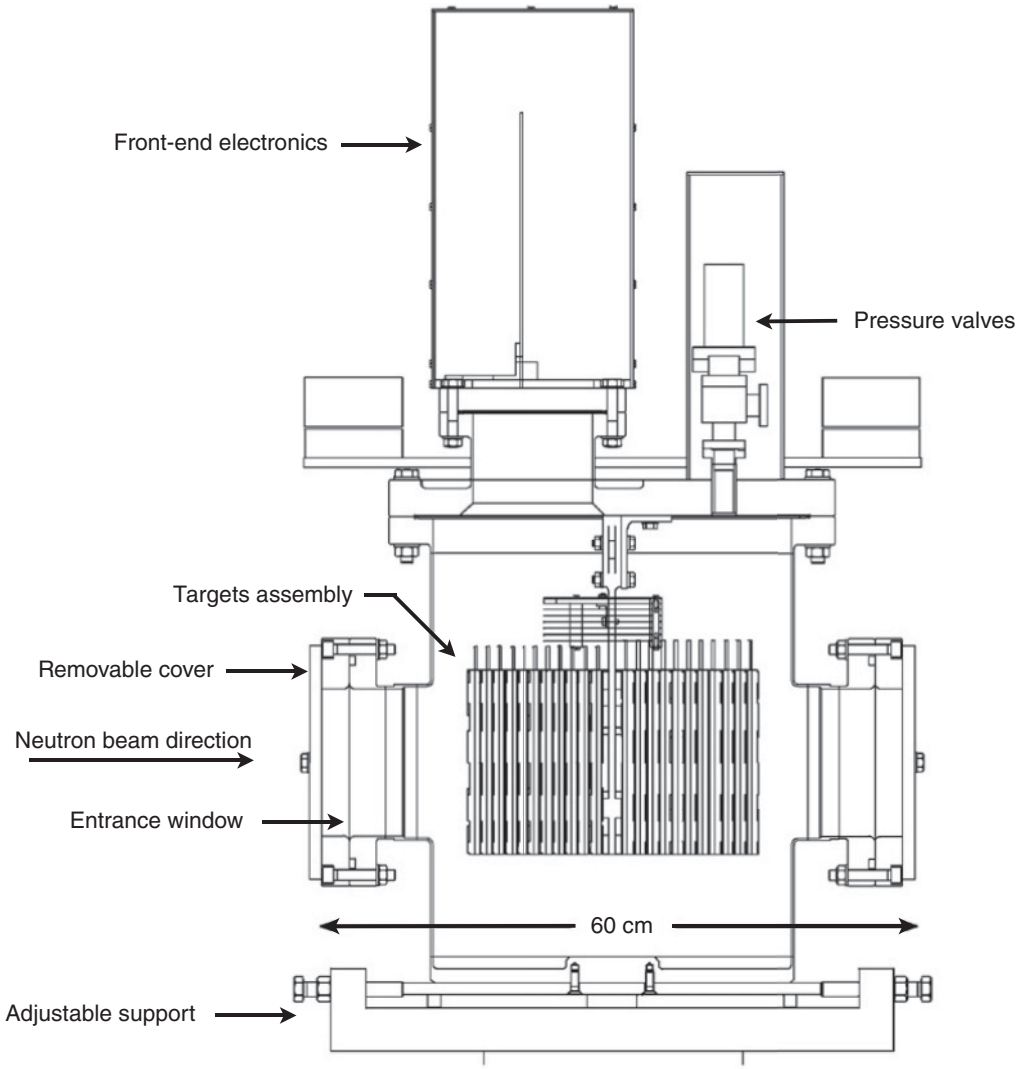

FIG. 1. Schematic view of the fast ionization chamber used for measuring the ^{236}U(n,f) cross section at n_TOF.

are listed in Table I. The ^{236}U samples were enriched to 99.85% with residual impurities of 0.05% ^{235}U and 0.1% ^{238}U. The α-particle activity of each ^{236}U sample at the time of the measurement was 8×10^{5} Bq. A remeasurement of the masses of the ^{236}U samples via α spectroscopy was performed at National Technical University of Athens (NTUA) with Si surface barrier detectors using a ^{241}Am calibration source. The results of this new measurement gave masses in agreement with the declared values.

TABLE I. Characteristics of the samples used in the measurement.

Sample	Mass (mg)	Thickness (10^{-7} atoms/b)	Uncertainty (%)
^{235}U	16.7	8.51	1.1
^{235}U	18.9	9.64	1.1
^{236}U	5.82	2.95	1.3
^{236}U	5.33	2.71	1.4
^{236}U	5.25	2.67	1.4
^{236}U	4.95	2.51	1.4

III. DATA ANALYSIS

A. Signal reconstruction

A total of 1.4 TB of data was acquired using a total of 2.01×10^{18} protons on the spallation target during the 17 days of measurement. The digitized signals from CASTOR were reconstructed by means of C++ routines developed using the ROOT framework [30] and based on the Advanced Spectra Processing Function class TSpectrum. For each signal, the reconstruction routine returned the amplitude, integral, baseline, and time information in a procedure similar to other fission measurements at n_TOF [31,32]. For each neutron bunch, the time and intensity of the corresponding proton bunch was also recorded.

The amplitude spectrum of the signals integrated over the whole neutron-energy range is shown in Fig. 2, featuring the characteristic double-humped shape produced by the fission fragments and the low-amplitude peak contributed by α background and noise. The peak at high amplitudes is due to a saturation effect in the flash ADC, which was found to

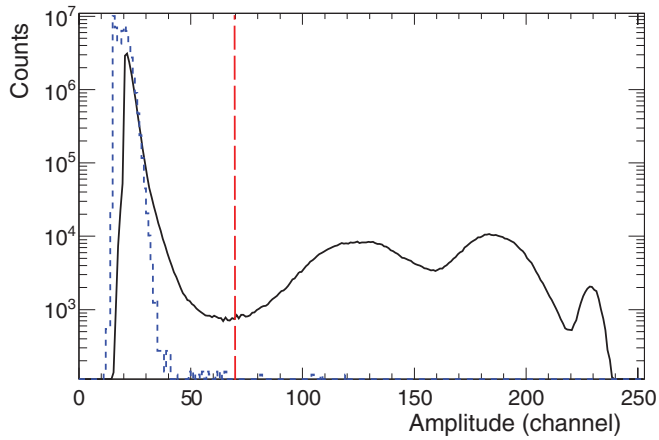

FIG. 2. (Color online) Amplitude spectrum measured from the ^{236}U electrodes. The black and blue (dashed) lines indicate the data taken with and without the neutron beam, respectively, normalized by the number of corresponding proton bunches. The amplitude threshold is set at channel 70 as indicated by the red (dashed) vertical line.

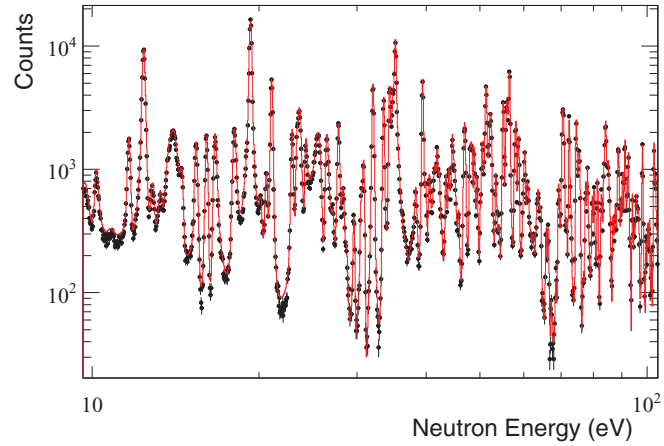

FIG. 3. (Color online) ^{235}U counts (black points, error bars corresponding to statistical uncertainties) as a function of neutron energy and the scaled standard ^{235}U(n,f) cross section from ENDF/B-VII.0 (red line). The very good agreement with the evaluated cross section in the resonance region confirms the correct neutron energy calibration.

be independent of rate. In the analysis of the ^{236}U as well as of the ^{235}U data, a software threshold was set at channel 70, corresponding to 35 MeV of deposited energy, to reject almost all events related to electronic noise and α-particle background. For this amplitude cut, the detection efficiency for fission fragments was calculated to be 97.1% and 90.2% for the ^{236}U and ^{235}U samples, respectively. Such accurate values concern the statistical uncertainty resulting from the FLUKA Monte Carlo simulations. The smaller detection efficiency in ^{235}U is explained by a larger thickness of the ^{235}U samples with respect to the ^{236}U samples, which results in an absorption of a larger fraction of fission fragments inside the ^{235}U samples, relative to the thinner ^{236}U samples.

B. Neutron-energy calibration

The neutron energy was calculated from the measured time of flight relative to the prompt signal produced by the γ flash (spallation γ rays and relativistic particles). The flight path distance was precisely calibrated by means of the resonances in the ^{235}U(n,f) cross section. Figure 3 shows the count rate as a function of neutron energy for the ^{235}U sample, compared to the evaluated cross sections of ENDF/B-VII.0 in a selected energy range. The excellent agreement obtained in this energy range confirms the correctness of the time-to-energy relation. The energy calibration of the ^{235}U sample was adopted for the ^{236}U sample by taking into account the physical distances between the samples.

C. Background subtraction

The fission yield of the ^{236}U(n,f) reaction is shown in Fig. 4 from the thermal neutron-energy range up to the fission threshold. The main sources of background are a residual contribution of α particles from the ^{236}U decay and fission events from the ^{235}U impurities in the ^{236}U samples.

The residual α-particle background was estimated from runs without the neutron beam, and was found to be negligible. On the contrary, the contamination from the ^{235}U(n,f) reactions is important, due to the much larger cross section of ^{235}U relative to ^{236}U (a difference of a factor of 10^4 in cross sections compensates an impurity in the sample of 5×10^{-4}). In fact, several ^{235}U resonances are clearly visible in the fission yield of the ^{236}U sample. Accordingly, the subtraction of the ^{235}U(n,f) component is crucial for the correct determination of the ^{236}U(n,f) cross section below the threshold and might have been responsible for the discrepancies among previous results. In the present analysis the correction for the ^{235}U(n,f) impurity was determined by analyzing the resonance at 8.79 eV, which is one of the biggest

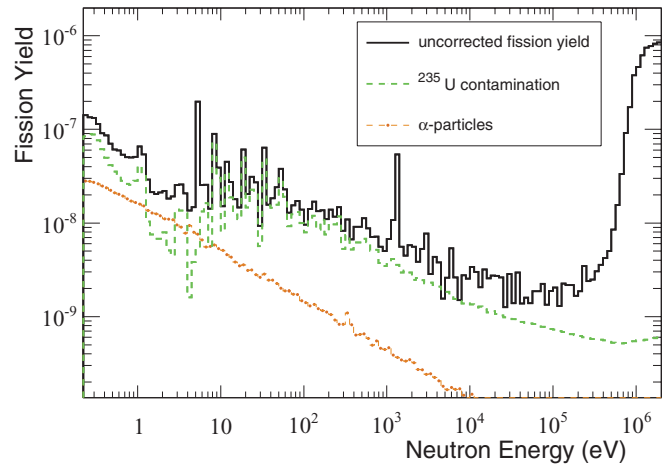

FIG. 4. (Color online) Fission yield measured with samples (black histogram), ^{235}U(n,f) yield normalized to the ^{235}U impurity (green dashed histogram), and the residual α-particle background (orange circles). The contribution of the ^{235}U contamination to the ^{236}U signal is evident in the region above the ^{236}U resonance at 5.45 eV.

TABLE II. Systematic uncertainties of the ^{236}U(n,f) cross section.

Source of uncertainty	Uncertainty (%)		
	170 meV to 1 keV	1 keV to 500 keV	500 keV to 2 MeV
Background subtraction	5.0	10.0	Negligible
Samples thickness	1.8	1.8	1.8
Efficiency correction	2.0	2.0	2.0
Dead-time correction	Negligible	Negligible	5.0
Normalization to ^{235}U(n,f)	2.0	1.0	1.0
Total	6.0	10.4	5.8

resonances in the ^{235}U(n,f) cross section. The analysis was performed under the assumption that the measured yield in this energy region is essentially all due to the ^{235}U contamination, with a negligible contribution from the ^{236}U(n,f) reaction, as suggested by the recent results with the higher-purity sample of Wagemans *et al.* [19] (in the uncorrected data of [19] the 8.79 eV resonance is a factor of 10 smaller than observed at n_TOF, as expected from the declared ^{235}U contamination). A fit of the observed resonance at 8.79 eV in the present data returned a value for the ^{235}U contamination of 0.043%, close to the declared value of 0.05%, thus providing further confidence in the method. The impurity determined in this way was then used to subtract the ^{235}U contribution from the measured yield over the entire energy region.

D. Cross-section determination

As a function of neutron energy the ^{236}U(n,f) cross section was determined with the ratio method, relative to the standard ^{235}U(n,f) cross section:

$$\sigma_{236} = \left(\frac{c_{236} - b_{236}}{c_{235} - b_{235}}\right)\left(\frac{N_{235}}{N_{236}}\right)\left(\frac{\varepsilon_{235}}{\varepsilon_{236}}\right)\left(\frac{\Delta_{235}}{\Delta_{236}}\right)\sigma_{235}^{\text{eval}}, \qquad (1)$$

where $c - b$ stands for the difference between the total number of counts and the background, both normalized to the same number of bunches, N is the sample thickness in atoms per barn, ε is the detection efficiency, Δ is the dead-time correction factor, and σ^{eval} stands for the evaluated ^{235}U(n,f) cross section, in this case taken from the ENDF/B-VII.0 library. The subscripts 235 and 236 refer to the uranium isotopes. The ratio method allows one to minimize systematic uncertainties; in particular, those related to the determination of the neutron flux, which cancels out in the cross-section ratio.

The efficiency corrections were evaluated by means of the FLUKA Monte Carlo simulations described in Sec. III. A threshold equivalent to the one on the measured amplitude spectrum of Fig. 2 was applied to the simulated spectrum of energy loss by fission fragments in the gas. The uncertainty on the efficiency correction, arising from the uncertainty in the sample thickness as well as on the amplitude-to-energy conversion used to estimate the threshold value, is estimated to be less than 2%. The dead-time correction was experimentally determined by the nonparalyzable model by looking at the time difference required for separating two consecutive signals, which was found to be 100 ns. Based on this value, the correction is at most 15% for ^{235}U in the energy range above 1 MeV, but always below 3% for ^{236}U due to the smaller sample mass and lower cross section. The uncertainty related to the dead-time correction is well below 1% for the subthreshold neutron-energy region, while it reaches an estimated 5% above 1 MeV, representing the biggest source of uncertainty in the high-energy region.

At low energy another source of uncertainty is related to the subtraction of the residual α-particle background and of the fission yield corresponding to the ^{235}U contamination in the sample. For the resonances reported here, the uncertainty in the kernel due to the background subtraction is below 5%, while the ^{235}U contamination has a larger influence in the region between 10 and 500 keV, where it accounts for at most half of the measured yield. In this energy region, propagating the uncertainty on the ^{235}U impurity yields an estimated uncertainty on the cross section of approximately 10%. A list of the various sources of systematic uncertainty and their contributions to the total cross-section uncertainty is given in Table II.

E. Resonance parameters

An analysis of the main resonances identified in this work was performed with the aim of extracting the fission width and comparing it with previous work and evaluations. The resonance fit was performed with the Bayesian code SAMMY [33] in the formalism of the multilevel Breit-Wigner formula. The resolution function of the neutron beam, Doppler broadening due to the thermal motion of the target nuclei as well as the finite size of the sample in single scattering, and self-shielding effects were taken into account in the analysis. Finally, the residual background, other than α particles and ^{235}U fission fragments, was assumed to be zero. The initial resonance parameters, as well as the spin and parity of the resonances used in SAMMY as input, were assumed from JENDL/AC-2008 [34]. While the energy and fission width of the resonances were left free during the fit, $\Gamma\gamma$ and Γ_n were kept fixed to the initial values.

IV. RESULTS AND DISCUSSION

A. Above thermal energy up to 5.45 eV resonance

The cross section of the ^{236}U(n,f) reaction was extracted from 170 meV to 2 MeV. The first resonance, which is also

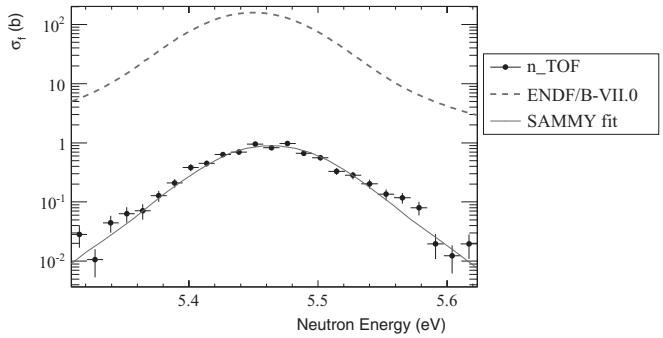

FIG. 5. (Color online) 5.45 eV resonance of ^{236}U(n,f) cross section, measured at n_TOF (black points, vertical error bars corresponding to statistical uncertainties) and the result of the SAMMY fit to the data (blue line) compared with the corresponding value in the ENDF/B-VII.0 library (red dashed line).

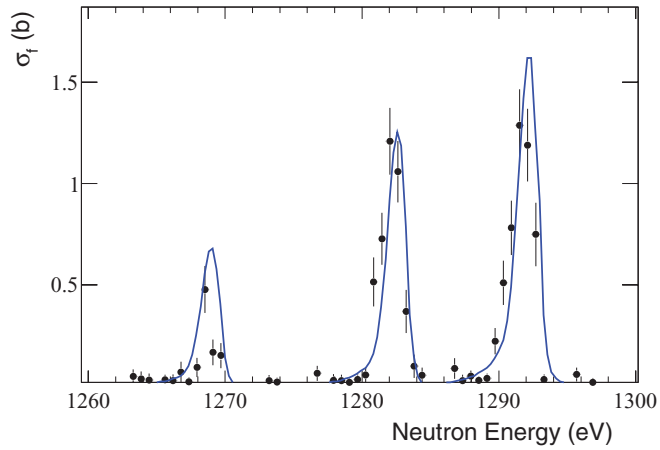

FIG. 6. (Color online) Resonance triplet at 1.25 keV was resolved at n_TOF with high resolution. The n_TOF data (black points, vertical error bars corresponding to statistical uncertainties) were fit with SAMMY (blue line).

the most important one below threshold, is at 5.45 eV. The calibration of neutron energy resulted in a slight shift of the first resonance with respect to previous measurements. The energy determined in this work by the SAMMY fit is 5.46 eV. The width of this resonance is found to be similar to the latest experimental values of Wagemans *et al.* [18,19] and Parker *et al.* [17] and to the evaluation of JENDL/AC-2008, which is based on these results. On the other hand, this resonance is overestimated in the ENDF/B-VII.0 evaluation by approximately a factor of 200, as shown in Fig. 5. This holds also for the cross section near thermal energies (at 170 meV in the present work), because the biggest contribution to the cross section at low energies comes from the tail of the 5.45 eV resonance.

B. Resonance and intermediate-energy region

As illustrated in Fig. 4, the fission yield of the ^{236}U sample prior to the removal of the ^{235}U contribution exhibits several resonances from 8 eV up to approximately 100 eV, but all these resonances disappear after subtracting the ^{235}U(n,f) background. The subtraction of the ^{235}U contamination also has the effect of substantially reducing the cross section below the first resonance, similar to the subtraction of the α background. After correction of the ^{235}U component, there are only a few resonances, which can be unambiguously attributed to the ^{236}U(n,f) reaction. Apart from the first resonance at 5.45 eV, a cluster of three narrow resonances is found around 1.25 keV, as shown in Fig. 6. This triplet has already been observed in previous data [17,19], but with less resolution, corresponding to class-II states with weak mixing [17].

The results of the resonance analysis are shown in Figs. 5 and 6, and the resonance parameters are reported in Table III. The fission width and kernel determined in this work are compared with the ones determined in the most recent measurements and with the latest evaluation of JENDL/AC-2008. In all cases, a reasonable agreement between various data sets and evaluations is observed for the 5.45 eV resonance (note that the fission width for this resonance in ENDF/B-VII.0 is still overestimated by two orders of magnitude). The new value for the fission width obtained from fitting the present data with SAMMY is compatible, within the estimated uncertainty, with the fission width provided by the JENDL/AC-2008 evaluation. In fact, a similarly good "fit" of the measured resonance is

TABLE III. Resonance parameters determined from the n_TOF data compared with values determined in previous work and in the latest evaluation. No uncertainty in $\Gamma\gamma$ and Γn was assumed when calculating the uncertainty in the kernel.

Resonance	n_TOF		Parker *et al.*		Wagemans *et al.*		Alekseev *et al.*		JENDL/AC-2008	
Energy			[17]		[18,19]		[20]		[34]	
	Γ_f (meV)	Kernel (meV)	Γ_f (meV)	Kernel (meV)	Γ_f (meV)	Kernel (meV)	Γ_f (meV)	Kernel (meV)	Γ_f (meV)	Kernel (meV)
5.45 eV	(1.6±0.2) $\times10^{-3}$	(6.9±1.0) $\times10^{-5}$	(1.3±0.1) $\times10^{-3}$	5.7×10^{-5}	(1.7±0.1) $\times10^{-3}$	6.9×10^{-5}	(1.05±0.1) $\times10^{-3}$	4.4 $\times10^{-5}$	(1.8±0.1) $\times10^{-3}$	7.7 $\times10^{-5}$
1.269 keV	2.3±0.7	(1.8±0.6) $\times10^{-1}$	0.82±0.03	6.8×10^{-2}					0.82±0.03	6.8 $\times10^{-2}$
1.282 keV	7.7±1.5	(3.5±0.9) $\times10^{-1}$	7.7±5	3.5×10^{-1}			2.0±0.32	7.6 $\times10^{-1}$	7.7±5	3.5×10^{-1}
1.292 keV	1.2±0.2	(5.1±1.0) $\times10^{-1}$	0.93±0.11	4.0×10^{-1}					0.93±0.11	4.0 $\times10^{-1}$

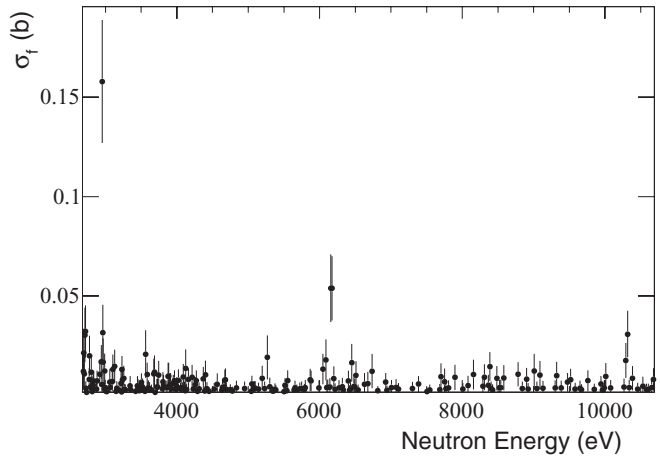

FIG. 7. Fission cross section of ^{236}U above 2 keV. The dominant resonances are at energies of 2.95 and 6.17 keV, but a weaker resonance is also shown at 10.3 keV.

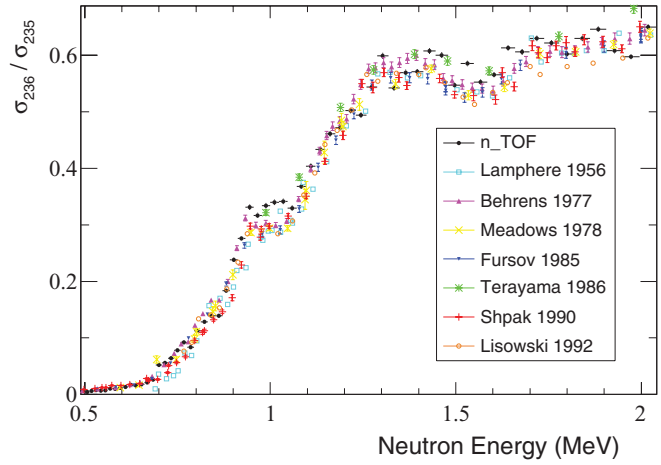

FIG. 9. (Color online) Fission cross-section ratio of ^{236}U and ^{235}U above threshold. The n_TOF results are plotted together with experimental data available from the EXFOR database [9,14,15,21–24].

obtained by fixing the Γ_f to the value of JENDL/AC-2008. For the triplet, the n_TOF resonance analysis can be compared only with the results of Parker *et al.* [17], since the resolution in the other two measurements was too poor to allow a resonance analysis for the three resonances separately.

The n_TOF results confirm the energy and strengths of the three resonances in the JENDL/AC-2008 evaluation. Among the additional resonances at energies of 2.95 keV, 6.17 keV and 10.3 keV shown in Fig. 7, an additional resonance at 36.5 keV has been observed. For these resonances, the low statistics available in the present data does not allow a reliable resonance analysis.

While below 1 keV the cross-section pattern is now well established, a large uncertainty persists in the region from a few keV up to the fission threshold. Few data have been collected in that region with sufficient accuracy, and current evaluations show large discrepancies between them. The main problem in this region is related to the contamination of ^{235}U in the sample, which has to be properly identified and subtracted. The results obtained at n_TOF, after determining and subtracting the yield related to the ^{235}U(n,f) contamination, as discussed in Sec. III C, are shown in Fig. 8. The present data are compared with the latest evaluations. As expected, ENDF/B-VII.0 clearly overestimates the cross section, up to 100 keV, by as much as a factor of 10, while JENDL/AC-2008 are well below the n_TOF results in the tens-of-keV region, contrary to the previous version JENDL-3.3 which was overestimating it in the same region. A remarkable agreement is observed instead for the latest release of JEFF-3.1 in the whole energy region, although some improvement could be possible around the threshold, where it shows some structures in the cross section, which are not observed in the present work (although the large binning used in the plot for the n_TOF data could partially mask those structures).

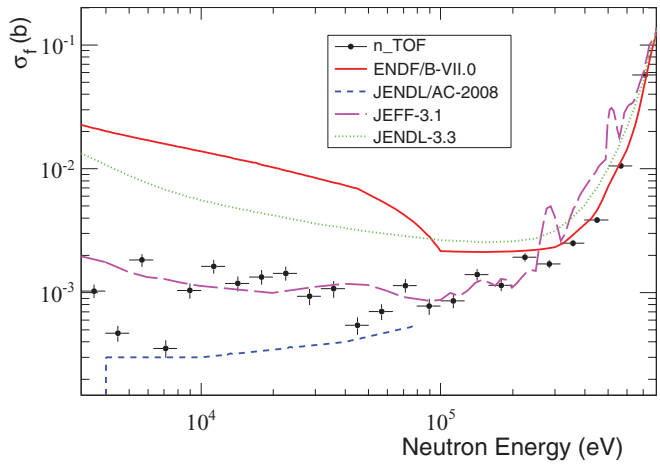

FIG. 8. (Color online) Cross section measured at n_TOF (black points) below threshold compared with evaluated data from ENDF/B-VII.0 (red line), JEFF-3.1 (purple long-dashed line), JENDL-3.3 (green pointed line), and JENDL/AC-2008 (blue short-dashed line) libraries.

C. Energy region above threshold

The present status of the cross section above threshold is satisfactory. Several measurements have been performed in the past, with a reasonable accuracy, showing generally a good agreement between each other. As a consequence, the evaluated cross section above 500 keV does not present anomalies, although there are differences in the fine structure between different libraries. Therefore, the n_TOF data are not expected to lead to much improvement in the current knowledge of the cross section in this high-energy region. Nevertheless, the data have been analyzed up to 2 MeV, in order to verify the accuracy of the present results, while providing at the same time additional data for improving fission models and related parameters. The results above the threshold at 690 keV for the fission cross-section ratio of ^{236}U and ^{235}U are shown in Fig. 9, together with several previous results [9,14,15,21–24]. The values of the ^{236}U(n,f) cross section above threshold are also given in Table IV, with a resolution of 100 bins per decade. As expected, on average the present results show a good agreement with previous data.

TABLE IV. Binned ^{236}U(n,f) cross section from 10 keV up to above the fission energy threshold.

E_{low} (keV)	E_{high} (keV)	σ (b)	Statistical Uncertainty (%)	E_{low} (keV)	E_{high} (keV)	σ (b)	Statistical Uncertainty (%)
10.000	12.5893	0.00104	14.0	933.254	954.993	0.319	1.5
12.5893	15.8489	0.00163	12.8	954.993	977.237	0.390	1.4
15.8489	19.9526	0.00119	13.9	977.237	1000.000	0.378	1.4
19.9526	25.1189	0.00134	13.4	1000.000	1023.29	0.401	1.5
25.1189	31.6228	0.00143	12.9	1023.29	1047.13	0.407	1.5
31.6228	39.8107	0.000934	14.9	1047.13	1071.52	0.409	1.4
39.8107	50.1187	0.00108	15.4	1071.52	1096.48	0.394	1.4
50.1187	63.0957	0.000545	16.2	1096.48	1122.02	0.439	1.2
63.0957	79.4328	0.000703	14.7	1122.02	1148.15	0.482	1.2
79.4328	100.000	0.00114	12.4	1148.15	1174.90	0.518	1.1
100.000	125.893	0.000777	14.9	1174.90	1202.26	0.553	1.1
125.893	158.489	0.000858	12.9	1202.26	1230.27	0.567	1.0
158.489	199.526	0.00134	10.8	1230.27	1258.93	0.605	1.0
199.526	251.189	0.00115	10.3	1258.93	1288.25	0.597	1.0
251.189	316.228	0.00193	7.8	1288.25	1318.26	0.658	0.9
316.228	398.107	0.00170	7.5	1318.26	1348.96	0.728	0.9
398.107	501.187	0.00252	6.4	1348.96	1380.38	0.661	0.9
501.187	630.957	0.00387	4.4	1380.38	1412.54	0.696	0.9
630.957	645.654	0.0186	6.2	1412.54	1445.44	0.700	0.9
645.654	660.693	0.0170	6.6	1445.44	1479.11	0.747	0.8
660.693	676.083	0.0208	5.8	1479.11	1513.56	0.741	0.8
676.083	691.831	0.0239	5.3	1513.56	1548.82	0.678	0.8
691.831	707.946	0.0293	4.8	1548.82	1584.89	0.728	0.8
707.946	724.436	0.0581	3.5	1584.89	1621.81	0.690	0.8
724.436	741.310	0.0625	3.4	1621.81	1659.59	0.709	0.8
741.310	758.578	0.0714	3.2	1659.59	1698.24	0.770	0.8
758.578	776.247	0.0873	2.8	1698.24	1737.80	0.763	0.8
776.247	794.328	0.103	2.6	1737.80	1778.28	0.796	0.8
794.328	812.830	0.0933	2.7	1778.28	1819.70	0.788	0.8
812.830	831.764	0.125	2.4	1819.70	1862.09	0.765	0.8
831.764	851.138	0.143	2.4	1862.09	1905.46	0.802	0.7
851.138	870.964	0.155	2.2	1905.46	1949.84	0.825	0.8
870.964	891.251	0.156	2.2	1949.84	1995.26	0.779	0.8
891.251	912.011	0.208	1.9	1995.26	2041.74	0.767	0.8
912.011	933.254	0.272	1.6	2041.74	2089.30	0.835	0.8

Good agreement was also found for all major evaluations (the difference between ENDF/B-VII.0 and JENDL-3.3 up to 2 MeV is below 5%, while a slightly larger difference, still below 15%, is observed for JEFF-3.1). Some structures are observed at 1.01 MeV, 1.53 MeV, and 1.64 MeV, which could signal some interesting behavior of the fission barrier of the ^{237}U nucleus. Some further investigation on these structures, and their potential implications in the theoretical description of the fission channel of this nucleus is ongoing and will be the subject of a forthcoming presentation.

V. CONCLUSIONS

This work reports on a new high-accuracy and high-resolution measurement of the neutron-induced fission cross section of ^{236}U performed at the n_TOF facility. The results obtained at low energy, in particular near the thermal region and for the first resonance at 5.45 eV, confirm the most recent data, which provided evidence that the evaluated cross section in ENDF/B-VII.0 is overestimated by more than two orders of magnitude. Instead, good agreement is obtained with the evaluated cross sections in JENDL/AC-2008. The present data also indicate that several resonances in the ENDF/B-VII.0 evaluation below 1 keV are not related to ^{236}U fission. Resonance parameters have been extracted from the present data for the resonance at 5.45 eV and for the three well-separated resonances of a triplet around 1.2 keV. In the 10–500 keV neutron-energy region, the cross section measured at n_TOF indicates that all current evaluations need some revision in this energy region, with the exception of JEFF-3.1. Above the fission threshold, the n_TOF data agree with previous data sets and with current evaluations. Some fine structure is observed in the region around the fission threshold, whose accuracy and implications are now being investigated.

The results of this work cover a wide energy range and are important in a re-evaluation of the ^{236}U(n,f) cross section, including a detailed parameterization of the resonance region. These results should be used in the development of the next-generation nuclear reactors in emerging and innovative nuclear technology concepts.

ACKNOWLEDGMENTS

This work has been supported by the European Commission's 5th Framework Programme under contract number FIKW-CT-2000-00107 (n_TOF-ND-ADS Project). The corresponding author of this work wishes to acknowledge the support of the Portuguese Foundation for Science and Technology (FCT) through grant SFRH/BD/43811/2008.

[1] INDC International Nuclear Data Committee, *Summary Report of the Consultants' Meeting on Assessment of Nuclear Data Needs for Thorium and other Advanced Cycles, INDC(NDS)-408* (IAEA, Vienna, 1999).

[2] U. Abbondanno *et al.*, *Measurements of Fission Cross Sections for the Isotopes relevant to the Thorium Fuel Cycle, CERN-INTC-2001-025 INTC-P-145* (CERN, Geneva, 2001).

[3] M. B. Chadwick *et al.*, Nucl. Data Sheets **107**, 2931 (2006).

[4] A. Koning *et al.*, JEFF Report **21** (2006).

[5] K. Shibata *et al.*, J. Nucl. Sci. Technol. **39**, 1125 (2002).

[6] W. Nyer, *LAMS-938* (Los Alamos Scientific Laboratory, 1950).

[7] W. Nyer, *The Neutron-Induced Fission Cross Section of ^{236}U as a Function of Energy, LA-1258* (Los Alamos Scientific Laboratory, 1951).

[8] J. Wahl and R. Davis, *Fission Cross-Section Measurements, LA-1681* (Los Alamos Scientific Laboratory, 1954).

[9] R. Lamphere, Phys. Rev. **104**, 1654 (1956).

[10] R. Lamphere and R. Greene, Phys. Rev. **100**, 763 (1955).

[11] J. Cramer and D. Bergen, *Fission Cross Sections from Pommard, LA-4420* (Los Alamos Scientific Laboratory, 1970), p. 74.

[12] J. Theobald, J. Wartena, H. Weigmann, and F. Poortmans, Nucl. Phys. A **181**, 639 (1972).

[13] H. Rosler, F. Plasil, and H. Schmitt, Phys. Lett. B **38**, 501 (1972).

[14] J. Behrens and G. Carlson, Nucl. Sci. Eng. **63**, 250 (1977).

[15] J. Meadows, Nucl. Sci. Eng. **65**, 171 (1978).

[16] F. Manabe *et al.*, The Technology Reports of the Tohoku University **52**, 97 (1988).

[17] W. Parker, J. Lynn, G. Morgan, P. Lisowski, A. Carlson, and N. Hill, Phys. Rev. C **49**, 672 (1994).

[18] C. Wagemans, O. Serot, P. Geltenbort, and O. Zimmer, Nucl. Sci. Eng. **136**, 415 (2000).

[19] C. Wagemans, L. De Smet, S. Vermote, J. Heyse, J. Van Gils, and O. Serot, Nucl. Sci. Eng. **160**, 200 (2008).

[20] A. Alekseev *et al.*, Phys. At. Nucl. **71**, 1351 (2008).

[21] B. Fursov, M. Klemyshev, B. Samylin, G. Smirenkin, and Yu. Turchin, At. Energ. **59**, 827 (1985).

[22] H. Terayama *et al.*, *Measurement of Fast Neutron-Induced Fission Cross Section of ^{236}U, ^{237}Np and ^{243}Am Relative to ^{235}U from 0.7 to 7 MeV, Progress Report, NEANDC(J)-122/U* (1986).

[23] D. Shpak, G. Korolev, and Kh. Androsenko, At. Energ. **69**, 998 (1990).

[24] P. Lisowski, A. Gavron, W. Parker, A. Carlson, O. Wasson, N. Hill, in *Nuclear Data for Science and Technology*, ed. S. M. Qaim (Springer, Berlin, 1992), p. 732.

[25] S. Abramovich *et al.*, *European Collaboration for High-Resolution Measurements of Neutron Cross Sections between 1 eV and 250 MeV. CERN/SPSC 99-8 SPSC/P 310* (CERN, 1999).

[26] U. Abbondanno *et al.*, *CERN n_TOF Facility: Performance Report. CERN-INTC-2002-037 INTC-O-011* (CERN, 2002).

[27] M. Calviani *et al.*, Nucl. Instrum. Methods Phys. Res., Sect. A **594**, 220 (2008).

[28] A. Ferrari *et al.*, *fluka: A Multi-Particle Transport Code. CERN-2005-10 INFN/TC 05/11, SLAC-R-773* (CERN, 2005).

[29] U. Abbondanno *et al.*, Nucl. Instrum. Methods Phys. Res., Sect. A **538**, 692 (2005).

[30] R. Brun and F. Rademakers, Nucl. Instrum. Methods Phys. Res., Sect. A **389**, 81 (1997).

[31] M. Calviani, Ph.D. thesis, Universit'a Degli Studi di Padova (2009).

[32] M. Calviani *et al.*, Phys. Rev. C **80**, 044604 (2009).

[33] N. Larson, *Updated users' guide for sammy: multilevel R-matrix fits to neutron data using Bayes' equations. Technical Report, ORNL/TM-9179/7* (Oak Ridge National Laboratory, 2006).

[34] O. Iwamoto, T. Nakagawa, N. Otuka, S. Chiba, K. Okumura, and G. Chiba, Nucl. Data Sheets **109**, 2885 (2008).